Low motional impedance bulk acoustic resonators based on metamaterials

X. Rottenberg[*], R. Jansen[*], V. Rochus[*], B. Figeys[*,**], B. Nauwelaers[**] and H. A. C. Tilmans[*]

[*]IMEC v.z.w., Kapeldreef 75, B3001 Leuven, Belgium, Xavier.Rottenberg@imec.be
[**]K.U.Leuven, ESAT, Kasteelpark Arenberg 10, B3001 Leuven, Belgium

ABSTRACT

This paper presents the implementation of propagating acoustic metamaterials in electrostatically transduced Bulk Acoustic Resonators (BARs) to tune by design their characteristic properties. Novel in this paper is our focus on lowering the observed motional impedance (R_m), key parameter for the design of low phase noise oscillators based on these BARs. We report on the modelling, simulation (not presented in the abstract) and experimental verification of the implementation of periodic square patterns of square holes, i.e., vacuum/air inclusions, in order to decrease R_m for the first width extensional resonance mode of electrostatically transduced bar-type BARs. The R_m is proportional to the characteristic acoustic impedance of the resonator material, i.e., $\sqrt{(E_{eff}\rho_{eff})}$, where E_{eff} is the effective Young's modulus and ρ_{eff} the effective mass density of the resonator material. The larger the proportion of hole area in the equivalent metamaterial is, the lower ρ_{eff} and E_{eff} are, and the lower R_m is. In the theoretical limit of holes filling the whole area, E_{eff}, ρ_{eff} and R_m approach zero.

We report a measured linear dependency of R_m on ρ_{eff} and in particular demonstrate metamaterial-based BARs with width and R_m respectively 1.5 smaller and 4 times lower than their natural bulk material counterparts.

Keywords: resonator, motional impedance, acoustic, metamaterial, effective parameter

1 INTRODUCTION

MEMS resonators are recognized as key components for emerging sensing, wireless and communications applications. Among those resonators, Si-based Bulk Acoustic Resonators (BARs), e.g., disks or bars, have recently gained special interest since they allow reaching high frequencies up to hundreds of MHz, while preserving a very high Q-factor of several thousands, and displaying a high linearity [1][2][3][4]. This type of resonators can further be produced through relatively simple processes like SOI (Silicon on Insulator), poly-silicon or poly-SiGe [5] based surface micromachining.

Figure 1 presents the top view of a typical bar-type BAR with T-shaped supports [1][2][3][4] implemented in imec's SiGe-based MEMS technology platform [5]. Not clearly visible in Figure 1 are the minute (sub-micron) membrane perforations or holes that are needed to release etch the structure. The extensional mode resonances for a "bar" resonator occur when an acoustic wave, trapped in the bulk of a parallelepipedic slab of material, bounces in phase on opposite faces. The frequencies f_{lmn} of the allowed extensional modes of vibration for a bar with dimensions W (width), L (length) and T (thickness) are given by [6]:

$$f_{lmn} \approx \frac{1}{2} v_{long}(E,\rho,\upsilon)\sqrt{\frac{l^2}{W^2}+\frac{m^2}{L^2}+\frac{n^2}{T^2}} \quad (1)$$

where E, ν, ρ and v_{long} are Young's modulus, Poisson's ratio, the mass density and the longitudinal acoustic phase velocity of the bar material, respectively. The integers l, m and n represent the mode numbers. Typically, in case of electrostatic transduction, the first width extensional mode of resonance f_{100} ($=v_{long}/2W=f_0$) is favored as the thin surface micromachined layers are not suited for an out-of-plane bulk mode excitation/detection, and moreover, the length can be used to increase the transduction efficiency without affecting the resonant frequency.

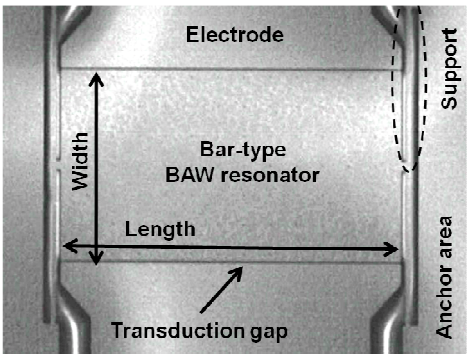

Figure 1 SEM of a bar-type BAR with T-support realized in imec's SiGe-based MEMS platform.

In a given technology, with fixed material properties, the design freedom is strongly limited. The designer can only change the dimension of the resonant direction of the bar (e.g., the width W) to reach the design goal, e.g., a certain width extensional resonant frequency. However, the effective properties of the material constituting a bar resonator can also be engineered by introducing holes (or macro-pores) to the bulk material [7][8][9]. These macro-porous materials behave like metamaterials which can be used to design non-homogeneous bar resonators, thus providing more design freedom.

This paper presents the implementation of propagating acoustic metamaterials in electrostatically transduced Bulk Acoustic Resonators (BARs) so as to tune by design their characteristic properties [10]. Novel in this paper is our focus on lowering the characteristic motional impedance (or

resistance) R_m. A low R_m is of crucial importance in the design of low phase noise oscillators based on these BARs. We report on the modelling, simulation and experimental verification of the implementation of periodic square patterns of square holes, i.e., vacuum/air inclusions, in order to decrease R_m for the first width extensional resonance mode of electrostatically transduced rectangular bar-type BARs.

2 MODEL

In this section, we present the model for a bar-type BAR and develop the concepts of a metamaterial which will lead to a shrinking of the BARs and a decrease of R_m .

2.1 Two-port bar-type BAR model

The measured transmission parameter, i.e., S-parameter S_{21}, of a typical SiGe-based 2-port bar-type BAR [4][5] around its first extensional mode resonance f_0, under three bias conditions is shown in Figure 2.

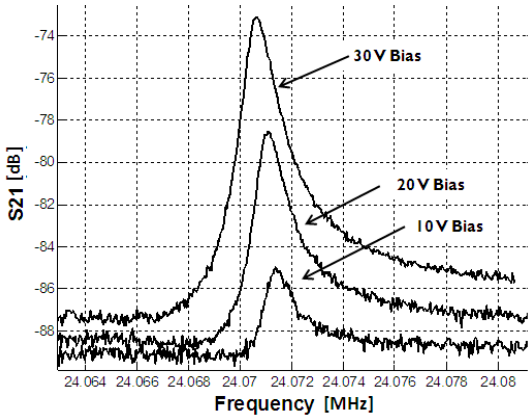

Figure 2 Typical measurement of the magnitude of S_{21} of a 100/200/4µm wide/long/thick SiGe BAR with gap spacings ~400nm under three bias voltage conditions.

The basic model of the device, neglecting the frequency-drift introduced by the electrostatic spring-softening, is shown in Figure 3(a). It consists of two purely electrical capacitances to ground, C_0, combined with the electric equivalent of an acoustic transmission line of acoustic length $\lambda/2$ at f_0. In the vicinity of its first width extensional resonance, the acoustic transmission line is approximated by two stages of RLC circuit as shown in Figure 3(b) with parameters given in eqns. (2)-(6), where the longitudinal velocity v_{long} is often approximated by $\sqrt{(E/\rho)}$, d is the width of the transduction gaps, V_{bias} is the amplitude of the bias voltage, Q_m denotes the quality factor of the resonance mode, C_m and L_m are the motional capacitance and inductance, respectively, and further, $\sqrt{(E\rho)}$ is recognized as the characteristic acoustic impedance of the resonator material [12][13]. Note that f_0 is linked to the ratio of E and ρ while R_m, through the reference impedance Z_{ref} , is linked to their product. Given a technology and build-up, f_0 fixes W and lowering of R_m is only possible through an increase of V_{bias} or L.

$$f_0 = \frac{1}{2W} v_{long} \approx \frac{1}{2W}\sqrt{E/\rho} \tag{2}$$

$$Z_{ref} = \frac{\pi d^4 \sqrt{E\rho}}{2V_{bias}^2 \varepsilon_0^2 WL} \tag{3}$$

$$R_m = \frac{Z_{ref}}{Q_m} \tag{4}$$

$$C_m = \frac{1}{2\pi f_0 Z_{ref}} \tag{5}$$

$$L_m = \frac{Z_{ref}}{2\pi f_0} \tag{6}$$

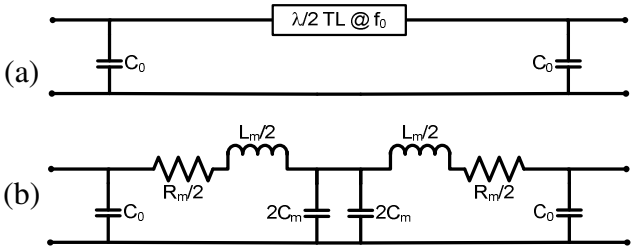

Figure 3 Equivalent circuit representations for the 2-port BAR shown in Figure 1: (a) a distributed transmission line of acoustic length $\lambda/2$ at f_0, and, (b) two lumped RLC equivalent circuits of acoustic length $\lambda/4$ at f_0.

2.2 Propagating metamaterials in BARs

The schematic top view of a bar-type BAR implementing a matrix of periodic holes aligned with the propagation direction of the longitudinal waves dominant in width extensional modes is shown in Figure 4.

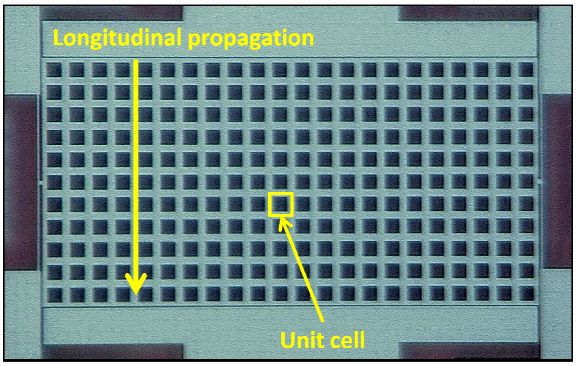

Figure 4 Top view microphotograph of a bar-type BAR with square pattern of square holes, realized in imec's SiGe-based MEMS technology platform [5].

Performing a virtual pull test on a unit cell of the considered metamaterial, we extracted in [10] the effective

material properties presented in Figure 5 and Figure 6, e.g., ρ_{eff} and E_{eff}. These effective parameters, used in eqns. (2)-(6) define the behaviour of a bar-type BAR implementing this family of metamaterials.

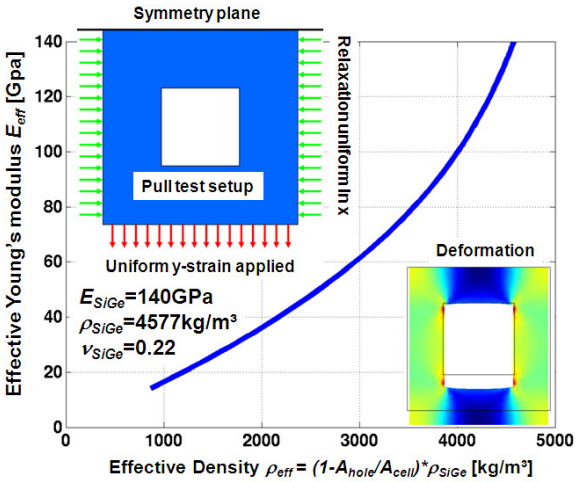

Figure 5 E_{eff} extracted from COMSOL simulations of static pull tests with relaxation and periodic boundaries.

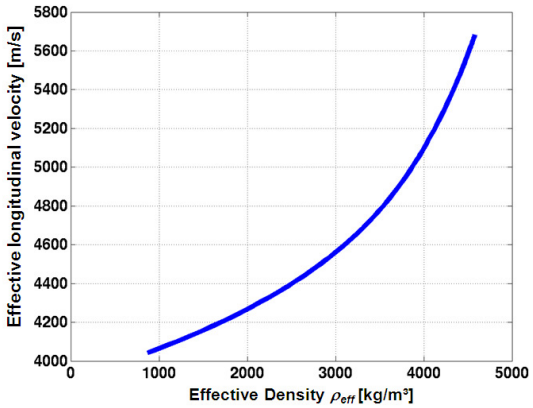

Figure 6 Effective $v_{long,\ eff}$ computed from COMSOL-extracted E_{eff} and ρ_{eff} as depicted in Figure 5 under the assumption that $v_{long,eff} = \sqrt{(E_{eff}/\rho_{eff})}$.

When ρ_{eff} drops to 0, E_{eff} does the same while the effective v_{long}, i.e. v_{long_eff} , remains non-zero. As a result, BARs from this family with equal W resonate at decreasing, but always non-zero, frequencies. Alternatively, at constant f_0, W can be shrunk. In comparison, R_m is proportional to the characteristic acoustic impedance of the resonator material and thus to $\sqrt{(E_{eff}\rho_{eff})}$. A lowering of ρ_{eff} results in a lower R_m. In the theoretical limit of holes filling the whole area, E_{eff} , ρ_{eff} and R_m approach zero. This trend is sketched in Figure 7 and appears to be close to a linear relationship. It is important to note that this R_m decrease is not solely due to a softening of the material but to the material becoming lighter as well.

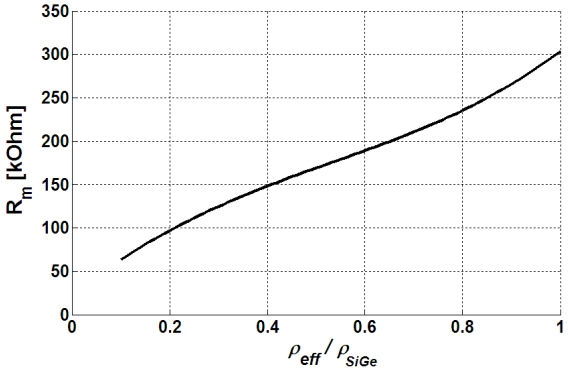

Figure 7 Effective R_m computed using eqns. (3) and (4) based on the ρ_{eff} and E_{eff} extracted from COMSOL, for BARs 55/110µm wide/long with 550nm wide transduction gaps, a constant Q_m= 20.000 and V_{bias}=140V.

3 EXPERIMENTAL VERIFICATION

We designed and characterized resonators from the family depicted in Figure 4 with identical overall geometries, differing only by their combination of hole size and pitch. Figure 8 reports the measured S_{21}–parameters close to the resonances. As the ratio of hole-area to total area increases, i.e., ρ_{eff} decreases, the resonance frequencies decrease and the peak height in the S_{21} magnitude increases.

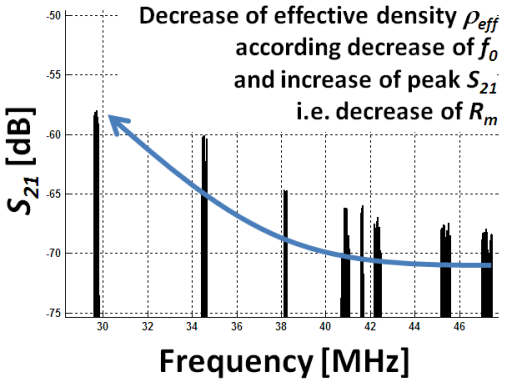

Figure 8 S_{21} measurements of devices of the type shown in Figure 4, 55/110/4µm wide/long/thick with 550nm wide transduction gaps and 140V bias voltage.

From these measurements, we extract both the effective longitudinal velocities as $2Wf_{res}$ and the effective R_m by fitting the model from Figure 3(b). Figure 9 compares the longitudinal velocities extracted from simulations and S_{21} measurements. These are in very good agreement, something which supports the theoretical non-nil limit of the resonance frequency decrease.

Figure 10 reports the measurement-based extracted R_m, which close to linearly decreases towards zero, in close agreement with the predictions from Figure 7. The discrepancy at $\rho_{eff}=\rho_{SiGe}$ is attributed to an actual

transduction gap narrower than assumed in simulations. The further departure from ideality observed in Figure 10 can further be explained by variations of actually measured Q-factors. Indeed, using these instead of the assumption of constant Q-factor, as in Figure 7, yields Figure 11 where the fine features from Figure 10 are clearly reproduced.

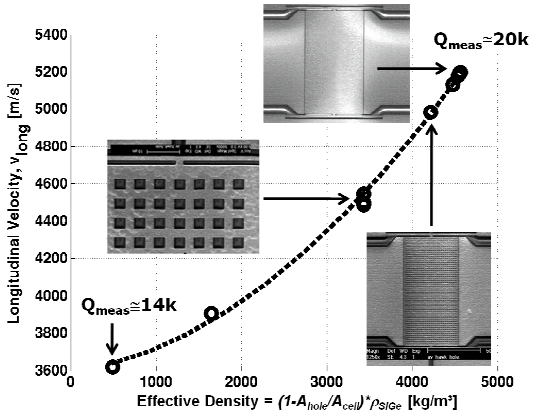

Figure 9 v_{long_eff} extracted from resonance frequency measurements of the type shown in Figure 8 vs. ρ_{eff}.

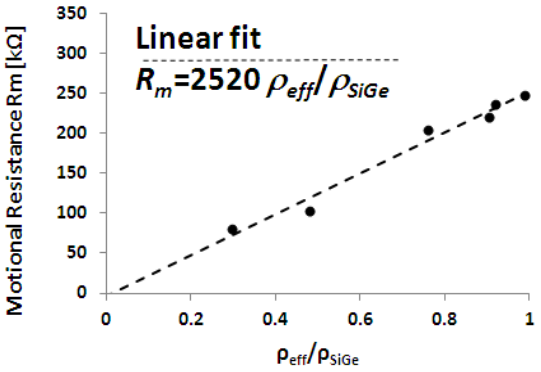

Figure 10 R_m (black dots) extracted from the measured S_{21} from Figure 8 vs. the normalized ρ_{eff}.

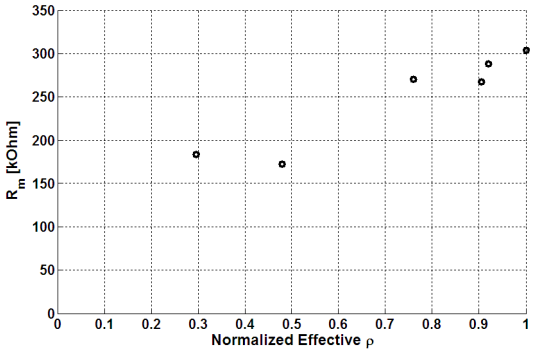

Figure 11 R_m simulated as in Figure 7 using the Q_m values extracted from measurements from Figure 8 vs. normalized ρ_{eff}.

4 CONCLUSIONS

This paper has presented the implementation of propagating acoustic metamaterials in BARs to tune by design their characteristic properties. We have demonstrated the possibility to not only shrink the BARs at constant frequency, but moreover to lower the motional impedance R_m at constant bias voltage. In particular we have demonstrated metamaterial-based BARs with width and R_m, respectively, 1.5x smaller and 4x lower than their natural bulk material counterparts.

REFERENCES

[1] S. Pourkamali, G. K. Ho and F. Ayazi, "Vertical Capacitive SiBARs", MEMS'05, pp. 211-214, Jan. 2005.

[2] J. Wang, Z. Ren, and C. T.-C. Nguyen, "1.156-GHz self-aligned vibrating micromechanical disk resonator," IEEE Trans. Ultrason., Ferroelect., Freq. Contr., vol. 51, no. 12, pp. 1607-1628, Dec. 2004.

[3] S. Stoffels, S. Severi, R. Vanhoof, R. Mertens, R. Puers, A. Witvrouw and H.A.C. Tilmans, "Light sensitive SiGe MEM resonator for detection and frequency tuning applications", MEMS'10, pp. 691-694, Jan. 2010.

[4] R. Jansen, S. Stoffels, X. Rottenberg, Y. Zhang, J. de Coster, S. Donnay, S. Severi, J. Borremans, M. Lofrano, G. vanderPlas, P. Verheyen, W. de Raedt and H.A.C. Tilmans, "Optimal T-Support Anchoring for Bar-Type BAW Resonators", proc. of MEMS'11, pp. 609-612, Jan. 2011.

[5] http://www.europractice-ic.com/MEMS_imec_SiGeMEMS.php

[6] H. J. McSkimin,"Theoretical analysis of modes of vibration for isotropic rectangular plates having all surfaces free" The Bell System Tech. J., Vol. 23, pp. 151-177, 1944.

[7] U. D. Larsen, O. Sigmund and S. Bouwstra,"Design and fabrication of compliant micromechanisms and structures with negative Poisson's ratio", J. MEMS, Vol. 6(2), pp. 99-106, 1997.

[8] P. Langlet, A. C. Hladky-Hennoin and J.-N. Decarpigny, "Analysis of the propagation of plane acoustic waves in passive periodic materials using the finite element method", J. Acoust. Soc. Am. Vol. 98, No.5, Pt.1, Nov.'95.

[9] S. Mohammadi and A. A. Eftekhar, "Acoustic band gap-enabled high-Q micro-mechanical resonators", Transducers '09, pp. 2330–2333, 2009.

[10] X. Rottenberg, R. Jansen, C. Van Hoof and H. A. C. Tilmans, "Acoustic meta-materials in MEMS BAW resonators", Appl. Phys A (2011) 103: pp. 869–875.

[11] X. Rottenberg, R. Jansen and H. A. C. Tilmans, "Phononic Bandgap coupled bulk acoustic wave resonators", proc. of MEMS'12, pp. 725-728, Jan. 2012.

[12] H. A. C. Tilmans, "Equivalent circuit representation of electromechanical transducers - Part II: Distributed-parameter systems", J. of Micromechanics and Microengineering, 7 (1997) pp. 285-309.

[13] V. Kaajakari, "Practical MEMS", Small Gear Publishing (March 17, 2009).